Pharmacodynamic biomarkers for anti-TIGIT treatment and prevalence of TIGIT expression in multiple solid tumor types

Fiore Cattaruzza, Pete Yeung, Min Wang, Alayne Brunner, Erwan Le Scolan, Yu-Wang Liu, Jennifer Cain, Gilbert O'Young, Gretchen Argast, Belinda Cancilla, Austin Gurney, Tim Hoey, John Lewicki, Ann M. Kapoun, OncoMed Pharmaceuticals, Inc., Redwood City, CA

INTRODUCTION

TIGIT (T cell immunoreceptor with Ig ITIM domain) is a co-inhibitory receptor of T cell and Natural Killer (NK) cell activity in the healthy immune system.

In tumors, TIGIT is highly expressed on a subset of dysfunctional T and NK cells and on highly suppressive regulatory T cells (Treg).

Loss of TIGIT signaling enhances NK cell activity, CD4+ T cell priming and CD8+ T cell effector functions, suggesting a role in anti-tumor immunity.

We have generated an anti-TIGIT IgG1 antibody, OMP-313M32, to stimulate anti-tumor immunity. As a murine surrogate for preclinical studies, we generated 313R12, an anti-TIGIT blocking antibody that showed dose-dependent, potent single agent antitumor efficacy in multiple syngeneic mouse models. Pharmacodynamic (PD) biomarkers in blood and in tumor were also identified, using flow cytometry, immunohistochemistry, and gene expression analysis.

Our preclinical biomarker data can be utilized to demonstrate target engagement for our clinical stage anti-TIGIT antibody, OMP-313M32.

MATERIALS AND METHODS

313R12 is a surrogate rabbit-mouse chimeric IgG2a monoclonal antibody that binds murine TIGIT (produced by OncoMed Pharmaceuticals).

Female Balb/c (4T1 and CT26.WT) or C57Bl/6J (B16F10) mice, 6-8 weeks old, were purchased from Envigo and Charles River Laboratories. The syngeneic models were developed from cells obtained from the American Type Culture Collection (Manassas, VA). After tumors were established, mice were randomized into treatment groups and dosed weekly (IgG2a, saline, and 313R12 at 0.1, 0.5, 2.5 or 12.5 mpk). Tumor measurements were performed twice a week. At the termination of the *in vivo* experiments, tumors, blood and spleens were harvested and processed for PD biomarker analysis.

Snap frozen tumor samples were processed using the RNeasy Fibrous Tissue Mini Kit (Qiagen, Valencia, CA), while whole blood RNA was isolated using the PAXgene Blood RNA kit. Total RNA from paired tumors and blood samples were isolated and analyzed using Affymetrix Mouse Genome 430 2.0 oligonucleotide microarrays (Affymetrix, Santa Clara, CA) at Almac Diagnostics (Craigavon, UK). qRT-PCR analysis was performed on a QuantStudio 7 Flex Real Time PCR System (Applied Biosystems/Thermo Fisher Scientific, Waltham, MA).

For flow cytometry, tumor samples were dissociated into single cell suspensions and incubated with cocktails of multiple antibodies for membrane markers or intracellular cytokines. Prior to staining for the detection of intra-cellular cytokines, cells were stimulated for 4 hours at 37°C in a CO_2 incubator with 50 ng/ml phorbol 12-myristate 13-acetate (PMA, Sigma, St. Louis, MO), 1 µg/ml ionomycin (Sigma, St. Louis, MO) in the presence of Monensin and Brefeldin A (eBioScience, San Diego, CA). When staining was completed, the cells were fixed with paraformaldehyde 1.6% (PFA, Alfa Aesar, Haverhill, MA). Data were acquired and analyzed on a Fortessa X20 flow cytometer using the FACS DIVA software (BD Biosciences, San Jose, CA).

For immunohistochemistry (IHC), TIGIT expression studies in human tumors and associated stroma and tumor infiltrating lymphocytes (TILs) were performed at QualTek Laboratories (Newtown, PA), using an anti-human TIGIT antibody generated at OncoMed Pharmaceuticals. IHC staining and quantification of Cd4 and Cd8 on murine tissue were performed at OncoMed.

For measuring NK cell cytotoxic activity, spleens were processed into a single cell suspension and cultured overnight. Cytotoxic activity was determined by adding calcein AM-labeled YAC-1 tumor cells to the splenocyte cultures for 4 hours and evaluating cell death by calcein AM detection in the culture supernatants using a spectrophotometer.

RESULTS

Anti-TIGIT treatment shows antitumor efficacy in multiple syngeneic models

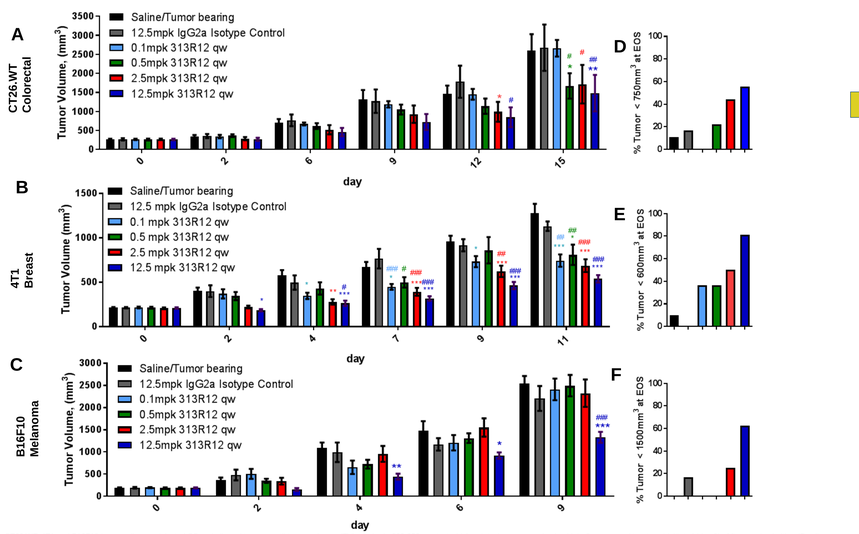

CT26.WT, 4T1 and B16F10 tumor cells were injected SC and allowed to grow until tumor volumes (TV) reached ~200-250 mm³, at which point mice were randomized into 6 groups and treatment initiated (day 0). Mice received either IP saline solution (black), IgG2a Isotype control (gray), or 313R12 (12.5mpk, blue; 2.5 mpk red; 0.5 mpk green and 0.1 mpk light blue). Mean±SEM, n=9-10 animals per group. *, **, *** indicate P<0.05, 0.01, 0.001 vs saline; #, ##, ### indicate P<0.05, 0.01, 0.001 vs IgG2a isotype control.

Panels A, B, and C show efficacy graphs of *in vivo* dose-response studies, demonstrating robust single agent antitumor activity on large established tumors from different syngeneic models.

Panels D, E, and F show the percentage of mice in each treatment group that had TV<750, 600 and 1500 mm³ at the end of study (EOS). These values of 750, 600 and 1500 mm³ were approximately half of the tumor volume in the control groups.

Anti-TIGIT treatment promotes activation of T and NK cells in the tumor

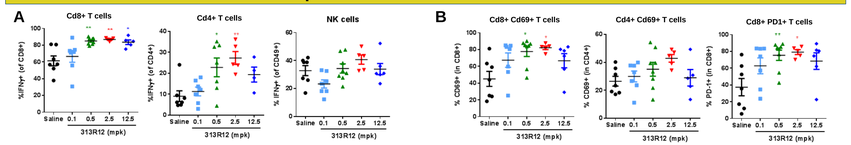

Each symbol corresponds to an individual animal. Saline (black circles), 0.1 mg/kg (mpk) 313R12 (blue squares), 0.5 mg/kg 313R12 (green triangles), 2.5 mg/kg 313R12 (red triangles), 12.5 mg/kg 313R12 (dark blue diamonds). Mean±SEM, n=6-7 animals per group. *, ** indicates P<0.05, 0.01, respectively, vs saline by one-way ANOVA followed by Dunnett's post test.

Panel A shows that increasing doses of anti-TIGIT stimulate dose-dependent IFNγ production from $Cd8^+$ and $Cd4^+$ T cells and NK cells.

Panel B shows that increasing doses of anti-TIGIT stimulate expression of activation (Cd69) and exhaustion (PD1) markers in tumor infiltrating leukocytes.

Anti-TIGIT treatment promotes infiltration of T cells into the tumor

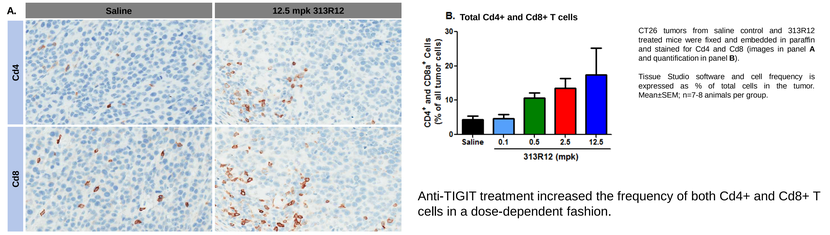

CT26 tumors from saline control and 313R12 treated mice were fixed and embedded in paraffin and stained for Cd4 and Cd8 (images in panel **A** and quantification in panel **B**).

Tissue Studio software and cell frequency is expressed as % of total cells in the tumor. Mean±SEM; n=7-8 animals per group.

Anti-TIGIT treatment increased the frequency of both Cd4+ and Cd8+ T cells in a dose-dependent fashion.

Anti-TIGIT treatment promotes NK cell cytotoxicity

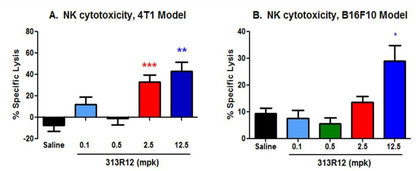

Results are expressed as % specific lysis, with Specific Lysis = (Experimental lysis – avg. minimum lysis) / (avg. maximum lysis – avg. minimum lysis)*100. Mean±SEM, n=6-7 animals per group. *, **, *** indicate P<0.05, 0.01, 0.001, respectively, vs saline by t-test.

Anti-TIGIT treatment promotes NK cytotoxic activity in a dose-dependent fashion in splenocyte cultures from mice bearing tumors from different syngeneic models.

Prevalence of TIGIT-expressing immune cells in human tissues

A Percentage of cases for each indication with TIGIT-Positive Immune Cell Abundance ≥2 in Tumor

Group	Tumor Indication	% of Cases with Abundance ≥2*
High when range = 30-100% of cases ≥2	TNBC	67%
	T-cell Lymphoma	50%
	H&N CA	35%
	Cervical CA	33%
Moderate when range = 10-29% of cases ≥2	Gastric CA	18%
	Melanoma	18%
	NSCLC Squam	15%
	Bladder CA	13%
	Ovarian CA	13%
Low when range = 0-9% of cases ≥2	Endometrial CA	8%
	RCC	7%
	Colon CA	4%
	NSCLC Adeno	4%
	Pancreatic CA	4%
	Esophageal CA	0%
	Leukemia	0%
	Prostate CA	0%

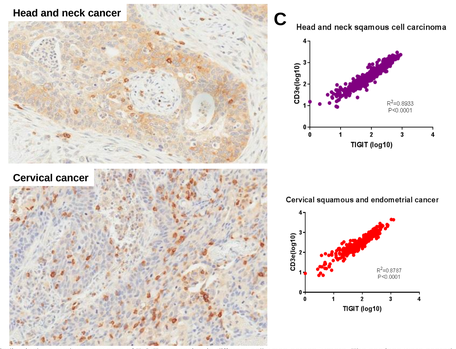

We generated a human anti-TIGIT antibody and profiled 17 cancer indications (~20 cases per indication), to evaluate patterns of TIGIT expression in different cell types across tumors. The sections were scored for TIGIT staining: 1) in tumor cells; 2) in immune cells associated with tumor tissue (panel **A**); 3) immune cells in the stroma.

Table in panel **A** shows the ranking of indications with high, moderate and low TIGIT-positive immune cells within each tumor type. Triple-negative breast cancer, cervical cancer, head and neck cancer and T cell lymphoma had the highest staining in both stroma and tumor infiltrating leukocytes (representative images for H&N and CE cancer in panel **B**). Consistent with IHC data, analysis of 33 tumor types in The Cancer Genome Atlas by RNA-Seq showed a good correlation of the expression levels of TIGIT and T cell markers (representative graphs showing correlation of TIGIT and CD3e in H&N squamous cell carcinoma and cervical squamous and endometrial cancer, Panel **C**), suggesting that TIGIT is mostly expressed on immune cells.

The overall incidence of TIGIT staining on the plasma membrane of tumor cells was infrequent and low intensity. Mining RNAseq data also showed low and infrequent TIGIT expression on tumor cells in a panel of 27 patient derived xenograft (PDX) models from OncoMed's tumor bank (data not shown).

Anti-TIGIT treatment induces PD changes in tumor

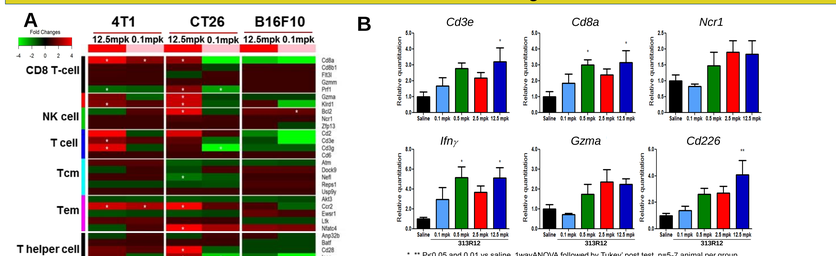

*, significantly regulated genes by the anti-TIGIT treatments with p-value <0.05 and absolute fold change ≥1.5 when compared to the saline group. n=3 representative animal per group.

*, ** P<0.05 and 0.01 vs saline. 1wayANOVA followed by Tukey' post test. n=5-7 animal per group.

Panel **A**: Microarray analyses of tumors shows immune cell-related gene changes induced by anti-TIGIT. 313R12 treatment promotes upregulation of genes associated with Cd8 and Cd4 T cells, NK cells, cell activation and cytotoxic activity, and Th1 cell response.

Panel **B**: qRT-PCR analysis confirmed anti-TIGIT dose-dependent increases of T cell and NK cell markers, as well as activation and cytotoxic activity markers.

Anti-TIGIT treatment induces PD changes in blood

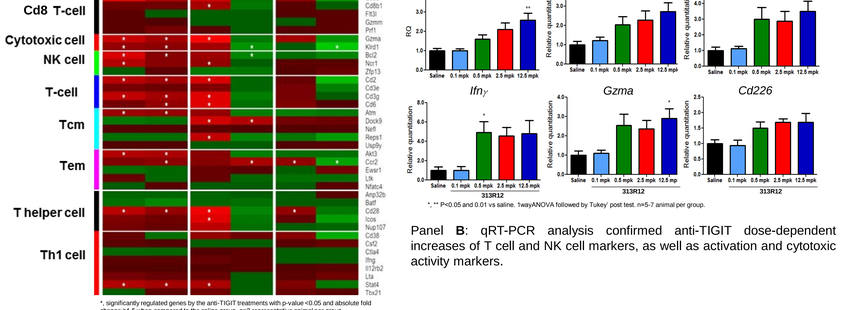

*, significantly regulated genes by the anti-TIGIT treatments with p-value <0.05 and absolute fold change ≥1.5 when compared to the saline group. n=3 representative animal per group.

*, ** P<0.05 and 0.01 vs saline. 1wayANOVA followed by Tukey' post test. n=5-7 animal per group.

Panel **A**: Microarray analyses of whole blood shows immune cell-related gene changes induced by anti-TIGIT in the periphery. Consistent with the tumor expression data, anti-TIGIT resulted in upregulation of genes associated with Cd8 and Cd4 T cells, NK cells, Th1 cell response as well as of markers of cell activation and cytotoxic activity.

Panel **B**: qRT-PCR analysis confirmed anti-TIGIT dose-dependent increases of T cell and NK cell markers, as well as activation and cytotoxic activity markers.

CONCLUSIONS

- Using a surrogate anti-TIGIT blocking antibody, we show potent single agent dose-dependent anti-tumor efficacy on large established tumors in multiple murine syngeneic mouse models.
- Anti-TIGIT treatment promoted a dose-dependent infiltration and activation of Cd8+ and Cd4+ T cells in the tumor microenvironment.
- Anti-TIGIT treatment increased NK cell activation in tumors and increased NK cell cytotoxicity in the spleen, which correlated with dose and efficacy.
- Consistent with the mechanism of action, anti-TIGIT treatment promoted upregulation of immune genes associated with activation of T and NK cells, Th1 response and cytotoxic activity. Results from blood and tumor were consistent, suggesting that blood may be a good surrogate tissue for measuring PD markers.
- IHC profiling of 17 tumor types to evaluate patterns of human TIGIT expression showed the highest TIGIT expression on immune cells associated with the tumor and in the stroma, while it was generally low on tumor cells.
- Using *in vivo* syngeneic mouse models, we have identified PD biomarkers in blood and in tumors that are consistent with the mechanism of action of anti-TIGIT. These biomarkers can be used in the clinic to demonstrate activity of anti-TIGIT antibody, OMP-313M32. A Phase 1a clinical trial of OMP-313M32 is planned for the first half of 2017.